VERIFICATION OF AN EXPERIMENTAL METHOD TO MEASURE THE STRESS-ELONGATION LAW FOR AN ADHESIVE LAYER USING A DCB-SPECIMEN

Tobias Andersson and Ulf Stigh

Department of Engineering Science, University of Skövde
P.O. Box 408, SE-541 28 Skövde, SWEDEN

ABSTRACT

A method to measure the stress-elongation law for a thin adhesive layer is presented. It is noted that the experimental results give a law that resemble the cohesive law that has been used *ad hoc* in general investigations of fracture and specifically in numerical simulations of adhesive bonds.

The method is based on the balance of energetic forces and a direct measurement of the elongation of the adhesive at the start of the layer. In the experiments, only the surfaces of the adherends are accessible for measurement. However, due to anticlastic deformation, the elongation at the interior is larger than at the surface. The method is also based on the assumption of linear elastic adherends. Influences of these prerequisites are studied using the finite element method.

Experimental and simulated results compare well up to the initiation of crack propagation. After this point, the simulations give, as expected, a constant J, while the experiments show a rapidly decreasing J. Similarly, the force-displacement records agree well up to the start of crack propagation. However, the experiments show a more rapidly decreasing force after this point than the simulations.

KEYWORDS

Thin layer, adhesive, test method, stress-elongation law

INTRODUCTION

Although of significant engineering importance, the design of adhesive joints is largely based on engineering practice and experimental verification. To this end, we suggest a design method based on finite element simulations using a constitutive law for the adhesive, c.f. [1,2,3,4].

In [5] Olsson and Stigh suggests a method to measure the stress-elongation relation for an adhesive layer. The method is based on the possibility to solve an inverse problem, namely to determine the stress-elongation relation for an adhesive layer in a DCB-specimen from measurable properties, see Figure 1.
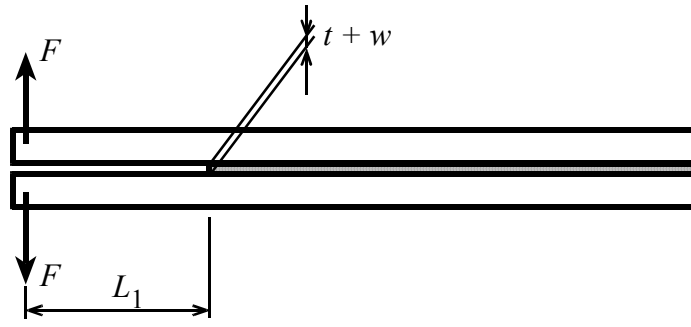
Figure 1: DCB-specimen

By continuously measure the applied force, F, the rotation of the points of load application, θ, and the elongation of the adhesive layer at its start, w, the stress-elongation relation is derived from

$$\sigma(w) = \frac{2}{b} \frac{\mathrm{d}\left(F\theta\right)}{\mathrm{d}w} \tag{1}$$

where b is the width of the specimen. In [5] Eqn. 1 is derived based on the assumption that the adherents behave as linear elastic Euler-Bernoulli beams. However, the relation is more general and in [4] the equation is derived based on the principle of balance of energetic forces. An energetic force is the energy-conjugated quantity corresponding to a change in position of an object[1]. Thus, the energetic force for a crack tip is known as the J-integral of the crack.

In [4] it is shown that the energetic force corresponding to an applied force, F, is the product of the force and the rotation, θ, of the loading point. Thus, $2F\theta$ is the applied energetic force, J_{applied}, of the specimen while $J_{\text{adhesive}} = \int_0^w \sigma(\tilde{w})\,\mathrm{d}\tilde{w}$ is the energetic force per unit width corresponding to the start of the adhesive layer, see [3,7]. If the specimen is long enough so that it can viewed as semi-infinite these two energetic forces must be in balance, see [4].

The experimental method is described in [4] and in more detail in [8]. Eqn. 1 incorporates a differentiation of the measured data. Different methods have been tested to evaluate the data. Originally, in [8], a simple numerical differentiation is used. A typical result is shown in Figure 2a. These curves end after about 30 to 40 μm. After this, the laser interferometric method used to measure w fail to operate. This is due to aliasing, see [4].
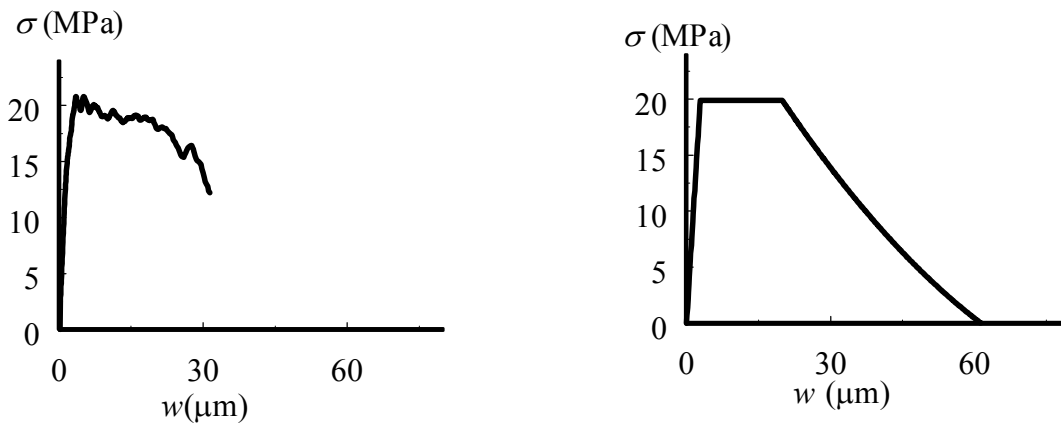

Figure 2: a) Typical result after numerical differentiation, b) The same data using the five-parameter curve

---

[1] The concept of an energetic force is introduced in solid mechanics by Eshelby [6] and can be viewed as the basis for Rice's J-integral [7].

Based on Fig. 4a and the corresponding curves of several experiments, a five-parameter curve is introduced in [4], see Figure 2b. The adjustment of this curve is done before the differentiation and under the condition that the area under the stress-elongation curve should equal the maximum $J_{applied}$ of the experiment. Thus, only four parameters are adjusted.

It is interesting to note the similarity with the stress-elongation law used by Tvergaard and Hutchinson in several numerical investigations of fracture, *e.g.* [9], and by Yang *et al*. [10] in simulations of fracture of adhesive joints. The difference between their *ad hoc* law and the present experimentally measured one is the form of the descending part. They use a linear relation while a parabolic relation adjusts better to the experimental data presented in [4]. As explained above, the form of the descending part is not fully captured in our experiments. However, the experimental data do not fit well to a linearly descending curve.

A prerequisite for the presented method is that no unloading takes place in the adhesive from a non-elastically deformed state. Another prerequisite is that no plastic deformation is allowed in the adherends throughout the experiment. These two requirements are examined here.

A shortcoming of the specimen is that only the surface is available for measurement of the elongation of the adhesive. Due to anticlastic deformation of the beams, the adhesive elongates more at the centre than at the surface of the specimen. Effects of this shortcoming are also examined.

CRITICAL EXAMINATION OF THE METHOD

The finite element method is used to simulate the experiments. In these simulations, the commercial program ABAQUS ver. 5.8 is used. The symmetry of the geometry and loading are utilised. Thus, only the upper adherend and the upper half of the adhesive layer are modelled. Beam elements (type B23) are used for the adherend and spring elements (type SPRING1) are used for the adhesive.

The total length of the adherend is 115 mm and the unbounded length is $L_1 = 50$ mm. The width is $b = 4.4$ mm and the height is $h = 5.5$ mm, for one adherend. The total thickness of the adhesive layer is nominally $t = 0.2$ mm.

The element size is determined in order to capture the gradients in the displacement field. This is done using an analytical solution [2] for the specimen with the stress-elongation curve as a saw-tooth, see Figure 3a. The stress-elongation curve is, in this case, described by three parameters; w_0, w_L and σ_0. To approximate the stress-elongation curve of Figure 2b we put w_0 equal to the elongation at the end of the linear elastic part of the curve, w_L equal to the maximum elongation and σ_0 equal to the maximum stress. From the analytical solution, we obtain the elastic part of the separation w along the adhesive, see Figure 3b. The strained region is about 20 mm long and 100 elements seem appropriate for this length. This gives 575 beam elements for the whole model. However, since the beam model is rather simple we finally chose 1000 beam elements, *i.e.* there are 1001 nodes in the model. This gives an element length of 0.115 mm which results in 566 spring elements.

The beams are made of steel with the yield strength larger than 450 MPa. In the finite element method, we use 206 GPa as the Young's modulus and 0.3 for the Poisson's ratio. The adhesive is modelled with springs. Except for the first spring, each spring element has a force-elongation relation according to $F = \sigma(w)l_e b$, where $l_e = 0.115$ mm is the beam element length along the adhesive layer and $b = 4.4$ mm is the width of the adherents. For the first element, only half of l_e is used.

As in the experiments, a simulation is done with a monotonically increasing displacement of the loading point.

To examine the difference between the simulations and the experiments the force vs. loading point displacement curves are first compared. Figure 4a shows the results from an experiment and a simulation of

the same experiment. From this curve, we can observe that the simulation corresponds well to the experimental result up to the maximum of the curve. The maximum force is in this case 84.1 N and from the simulation the maximum force is 86,8 N thus, an error of only 3 %. However, the maximum force is very sensitive to the length L_1 and some small differences exist between the test specimens. By varying L_1 a few tenths of a mm from the nominal value, a satisfying agreement can be achieved between the experiments and simulations for all experiments and for all curves, see Figures 4 and 5.
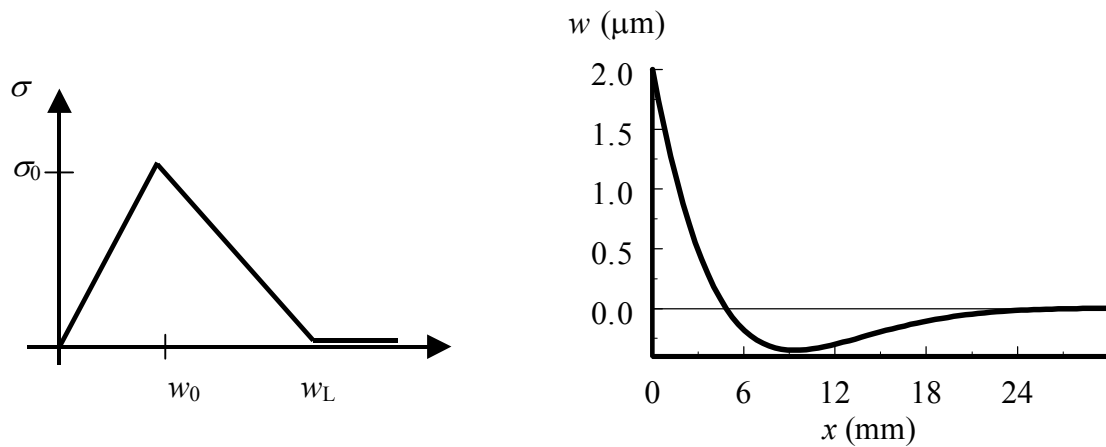

Figure 3: a) stress-elongation law used in analytical solution, b) elongation of adhesive along the specimen.

From Figure 4a, it is observed that the curves diverge soon after the maximum point is passed. The inserted line "critical displacement" indicates the value of the separations of the loading points corresponding to the maximum value of w; in this experiment 60 μm, see Figure 2b. As seen in Figure 4b, J still increases after this point. That is, the maximum elongation of the adhesive appears to be larger than the value derived from the adjusted curve. However, as soon as the maximum value of J is reached, J starts to decrease. This is not the case in the simulation. This can be attributed to the formation of a sharp crack within the adhesive layer when the crack starts to propagate. However, no recording of the start of crack propagation is done in these experiments.
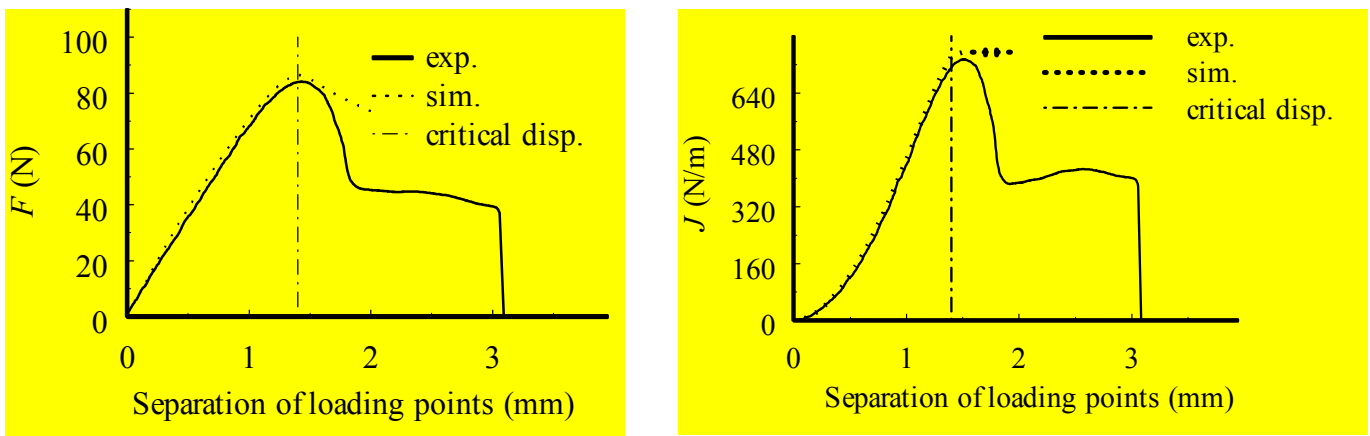

Figure 4: a) force vs. separation of loading points as recorded from a typical experiment and simulation; b) $J_{applied}$ vs. separation of loading points

Figures 5 show force vs. elongation and rotation vs. elongation respectively. Both curves agree well with the simulations, though one curve is consistently below and the other consistently above the experimental result.

The use of the present method is critically dependent on the assumption of a unique stress-elongation relation for the adhesive. This is not a realistic assumption for an adhesive; unloading from a severely deformed state is likely to take place along another path than the curve shown in Figure 2b. However, if the

4

adhesive experiences monotonically increasing or decreasing elongation during an experiment then the difference between a unique stress-elongation curve and the true one is without significance.
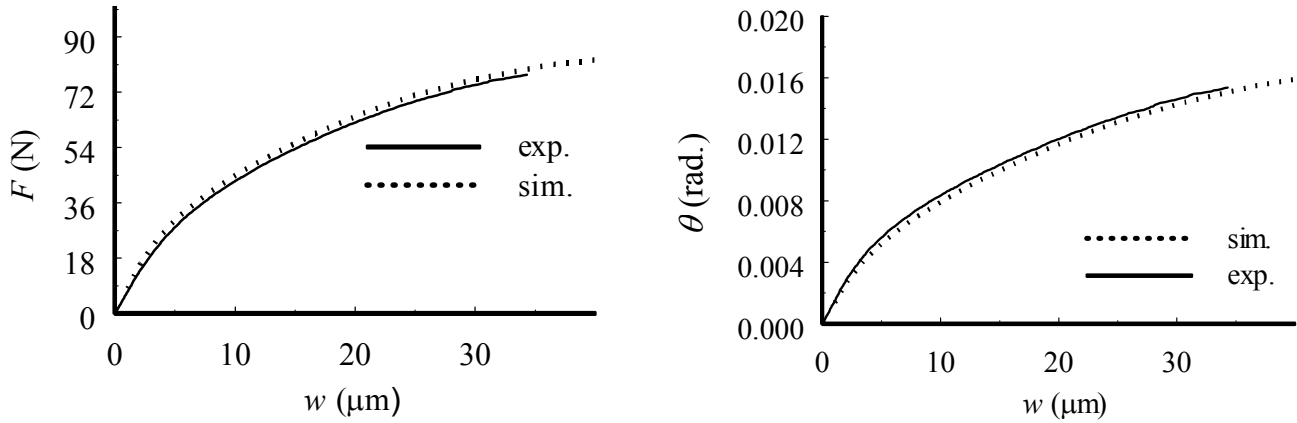

Figure 5: a) force vs. elongation; b) loading point rotation vs. elongation.

Figure 6 shows the elongation of the adhesive at consecutive points along the adhesive layer, the distance between the points is 2.3 mm. The first curve shows the elongation at the start of the layer. This part of the adhesive experiences a monotonically increasing elongation, as should be expected. Elements of the adhesive further inside the layer first experiences a compression, which is later followed by an elongation. The initial compression is understood from the well-known solution for a beam on an elastic foundation.
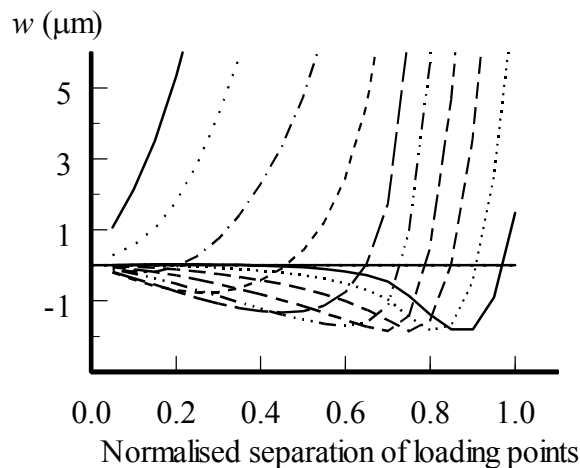

Figure 6: Elongation vs. normalised separation of loading points of different point of the adhesive according to simulation. Normalisation relative to the value corresponding to splitting of specimen.

The maximum compression of any element of the layer does not exceed 2 μm which corresponds to $\sigma_0 = 19.6$ MPa. Thus, no inelastic deformation is expected at any part of the layer before it starts to elongate. Moreover, no element of the adhesive experiences unloading from an elongated state before a crack starts to elongate. Thus, the use of a unique stress-elongation relation in the theoretical basis for the method is consistent with the results of the simulations.

The maximum beam bending stress from the simulations does not exceed 270 MPa. Considering the low peel stress (about 20 MPa) by which the adhesive affects the adherends it can be conclude that no plastic deformation takes place in the beam elements.

The influence of anticlastic bending is studied using the elementary beam bending theory, see [11]. Since the peel stress from the adhesive is small, its influence is neglected. The cross section of the lower beam is shown in Figure 7. The displacement u is given by

$$u(x,y) = -\nu\frac{x^2 - y^2}{2R} \tag{2}$$

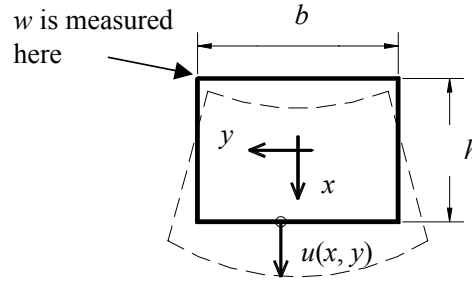where R is the radius of curvature of the beam given by $R = EI/M = EI/FL_1$.

Figure 7: Cross section of lower beam

The difference between u at the surface and at the interior is then given by

$$\delta = u\left(-\frac{h}{2}, \frac{b}{2}\right) - u\left(-\frac{h}{2}, 0\right) = \frac{\nu b^2}{8R} = \frac{4\nu bFL_1}{3Eh^3} \tag{3}$$

The total contribution to the separation w is 2δ. With the maximum force $F = 100$ N the maximum displacement $2\delta_{max} = 0.68$ μm is obtained. Comparing with the corresponding value of $w = 60$ μm the error is less than 1 %. Thus, it is possible to neglect the influence of anticlastic bending.

ACKNOWLEDGEMENTS

REFERENCES

1. Stigh, U. (1987). In: *Mechanical behaviour of adhesive joints*, pp 237-248, Verchery, G. and Cardon, A.H. (Eds.). Editions Pluralis, Paris, France.
2. Stigh, U. (1988). *International Journal of Fracture*, **37**, R13.
3. Alfredsson, K. A. and Stigh, U. (1997). In: *Advances in Fracture Research – Proceedings of ICF9*, pp. 2667-2674, Karihaloo, B. L., Mai, Y.-W., Ripley, M. I. and Ritchie, R. O. (Eds.). Pergamon, Amsterdam.
4. Stigh, U. and Andersson, T. (2000). In: *Fracture of polymers, composites and adhesives, ESIS Publication 27. Proceedings of the 2nd ESIS Conference*, Williams, J. G. and Pavan, A. (Eds.), Elsevier, Amsterdam.
5. Olsson, P. and Stigh, U. (1989). *International Journal of Fracture*, **41**, R71.
6. Eshelby, J. D. (1951). *Phil. Trans. R. Soc. London* **A244**, 87.
7. Rice, J. (1968). *Journal of Applied Mechanics* **35**, 379.
8. Andersson, T. (1998). MSc thesis, University of Skövde.
9. Tvergaard, V. and Hutchinson J.W. (1992). *Journal of the Mechanics and Physics of Solids*, **40**, 1377.
10. Yang *et al.* (1999). *Journal of the Mechanics and Physics of Solids*, **47**, 1337.
11. Goodier, J.N. and Timoshenko, S.P. (1970). *Theory of Elasticity*, McGraw-Hill, Singapore.